applied sciences

MDPI

Article

Deep Learning-Aided Downlink Beamforming Design and Uplink Power Allocation for UAV Wireless Communications with LoRa

Yeong-Rok Kim [1,†], Jun-Hyun Park [1,†], Jae-Mo Kang [1,*], Dong-Woo Lim [2,*] and Kyu-Min Kang [2]

[1] Department of Artificial Intelligence, Kyungpook National University, Daegu 41566, Korea; bohr74@knu.ac.kr (Y.-R.K.); wnsgus126@knu.ac.kr (J.-H.P.)
[2] Radio & Satellite Research Division, Electronics and Telecommunications Research Institute, Daejeon 34129, Korea; kmkang@etri.re.kr
* Correspondence: jmkang@knu.ac.kr (J.-M.K.); window0508@etri.re.kr (D.-W.L.)
† These authors contributed equally to this work.

Abstract: In this paper, we consider an unmanned aerial vehicle (UAV) wireless communication system where a base station (BS) equipped multi antennas communicates with multiple UAVs, each equipped with a single antenna, using the LoRa (Long Range) modulation. The traditional approaches for downlink beamforming design or uplink power allocation rely on the convex optimization technique, which is prohibitive in practice or even infeasible for the UAVs with limited computing capabilities, because the corresponding convex optimization problems (such as second-order cone programming (SOCP) and linear programming (LP)) requiring a non-negligible complexity need to be re-solved many times while the UAVs move. To address this issue, we propose novel schemes for beamforming design for downlink transmission from the BS to the UAVs and power allocation for uplink transmission from the UAVs to the BS, respectively, based on deep learning. Numerical results demonstrate a constructed deep neural network (DNN) can predict the optimal value of the downlink beamforming or the uplink power allocation with low complexity and high accuracy.

Keywords: beamforming design; convex optimization; deep learning; LoRa (long range); UAV (unmmaned aerial vehicle)

check for updates

Citation: Kim, Y.-R.; Park, J.-H.; Kang, J.-M.; Lim, D.-W.; Kang, K.-M. Deep Learning-Aided Downlink Beamforming Design and Uplink Power Allocation for UAV Wireless Communications with LoRa. *Appl. Sci.* **2022**, *12*, 4826. https://doi.org/10.3390/app12104826

Academic Editor: Christos Bouras

Received: 18 April 2022
Accepted: 8 May 2022
Published: 10 May 2022

1. Introduction

Unmanned aerial vehicle (UAV) wireless communication has attracted a lot of attention in both academia and industry thanks to a lot of advantages (e.g., alleviating the limitation of the locality, reaching hazardous area, controllability, etc.) [1–3]; that is, it can provide a dynamic wireless access wherever one need. However, a critical practical concern for the UAV wireless communication is to realize a long range communication, which however is limited in practice due to the limited battery life, as well as low energy efficiency of the UAV. In addition, when multiple UAVs exist in practice, there might be crosstalk or interference that would further degrade the communication performance. To address these issues, we leverage the LoRa (Long Range) [4] modulation with a proper transmission technique (such as beamforming or power allocation) for the UAV wireless communication, which is the first attempt in the literature to the best of our knowledge.

LoRa is one of the most popular and widely adopted low-power wide-area network (LPWAN) technologies developed for Internet-of-Things (IoT), because it enables long-distance communication with high battery/energy efficiency [5,6]. Additionally, the transmission technique, such as beamforming or power allocation, is even synergetic when combined with LoRa, because if properly designed or optimized, the received signal power can be further enhanced (and, thus, enables a much longer communication). In the literature [7–12], several beamforming or power allocation schemes were developed

for the non-UAV (i.e., traditional terrestrial) wireless communication based on the convex optimization-based approaches. Although these schemes can be extended to the UAV wireless communication (this will be presented in Section 2 as performance benchmarks for the proposed scheme), they generally require very high computational complexities, which is prohibitive in practice or even infeasible at the UAVs with limited computing capabilities, because the corresponding convex optimization problems (such as second-order cone programming (SOCP) and linear programming (LP)) requiring a non-negligible complexity need to be re-solved many times while the UAVs move. To address this critical complexity issue, an innovative and effective solution is urgently required. This motivated our work.

In this paper, we consider a UAV wireless communication system where a base station (BS) equipped multi antennas communicates with multiple UAVs, each equipped with a single antenna, using the LoRa modulation. In this system, we propose novel and efficient schemes for beamforming design for downlink transmission from the BS to the UAVs and power allocation for uplink transmission from the UAVs to the BS, respectively, based on a deep learning (DL). To address the aforementioned complexity issue effectively and intelligently, we construct a deep neural network (DNN), such that the optimal value of the downlink beamforming or the uplink power allocation can be predicted very efficiently based on the channel state information (CSI). Numerical results demonstrate the effectiveness and efficiency of the proposed scheme.

The remainder of this paper is organized as follows; The related work is described in Section 1.1. The system model and problem formulation are described in Section 1.2. The convex optimization-based conventional approaches and the proposed deep learning approach are presented in Section 2. The simulation results are presented in Section 3, and the paper is concluded in Section 4.

Notations: Boldface upper and lower case letters are used to denote matrices and vectors, respectively. $\exp(\cdot)$ denotes an exponential function. The transpose of vectors and matrices is denoted by $(\cdot)^T$, and we use $(\cdot)^H$ to denote Hermitian transpose. Additionally, $\|\cdot\|$ and $\preccurlyeq$ are used for denoting the Euclidean norm of vectors and component-wise inequality, respectively. In addition, $\mathrm{Re}(\cdot)$ and $\mathrm{Im}(\cdot)$ denote real and imaginary parts of a complex number, respectively. Additionally, $\mathcal{CN}(0, \sigma^2)$ denotes the distribution of a circularly symmetric complex Gaussian random variable with zero mean and variance σ^2.

1.1. Related Work

In [7], the authors only considered the transmitter optimization problem for a multiuser downlink channel with multiple transmit antennas at the BS, however, they did not leverage the DNN. Additionally, in [8,9], the optimal beamforming design was derived based on optimization theory. However, they did not consider the LoRa modulation and the DL. Additionally, the optimization theory based power allocation scheme was developed in [10–12], however, they also did not consider the LoRa modulation and the DL. In [13,14], the authors considered the optimal beamforming problem via deep learning, but they did not deal with the LoRa modulation. In [15], the authors used the beamforming technique in the LoRa-based sensing system. However, this work did not mention the method for designing the optimal beamforming vector. To the best of our knowledge, for the LoRa modulation signal, the deep learning based beamforming design or power allocation scheme has not been investigated in the literature.

1.2. System Model and Problem Formulation

We consider a UAV wireless communication system where multiple UAVs, each equipped with a single antenna, communicate with the BS equipped with multiple antennas. In this paper, we adopt the LoRa as means of wireless communications between the UAVs and the BS. Additionally, we consider both scenarios of the downlink and the uplink communications from the BS to the UAVs and from the UAVs to the BS, respectively, which are shown in Figure 1.

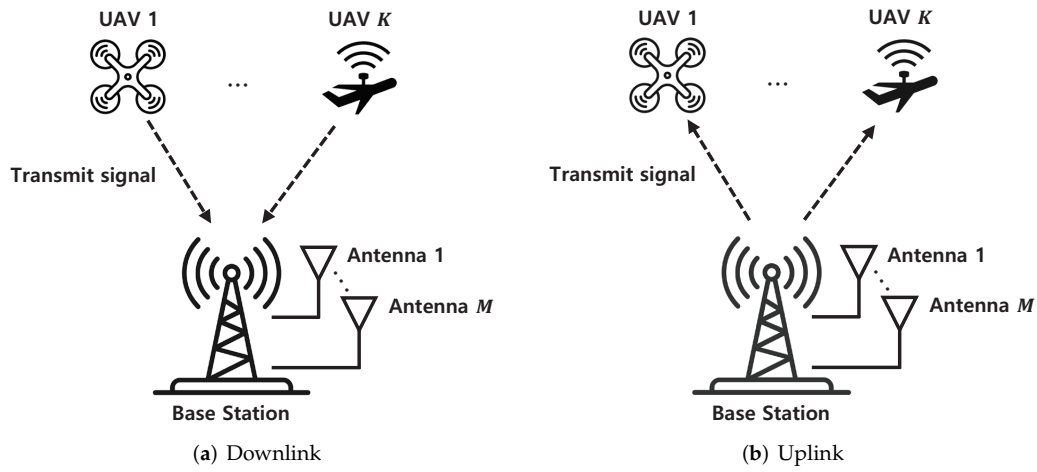

Figure 1. System models for UAV wireless communications.

1.2.1. LoRa

The LoRa is one of the widely adopted LPWAN technology for the Internet-of-Things (IoT) that uses chirp spread spectrum as a modulation scheme [5]. The LoRa modulated signal is capable of detecting symbols correctly (i.e., conducting successful communications) with a high probability even when the SINR is low [16], which, in turn, enables realizing long range communication. Furthermore, the LoRa modulation technique is known to be more robust to frequency/time-selective channel and multipath fading circumstances than conventional modulation methods such as frequency-shift keying [17]. Due to these benefits, in this paper, we adopt the LoRa as a means for the wireless communications between the BS and UAVs.

The LoRa modulated signal is in the form of a sinusoidal wave (i.e., a chirp wave) in which the frequency increases or decreases linearly with time until it achieves the nyquist frequency of $B/2$ or $-B/2$, where B represents the bandwidth [18]. The LoRa system supports bandwidths of 125 KHz, 250 KHz, and 512 KHz, as well as a spreading factor (SF) of 7–12. In the LoRa modulation, there are 2^{SF} different symbols in total, each of which is allocated different initial frequency values, where $SF \in \{7, \cdots, 12\}$ denotes the SF [6]. The LoRa modulated signal with symbol $s \in \{0, 1, \cdots, 2^{\mathrm{SF}} - 1\}$ in the continuous-time domain is defined as [19–21]

$$x_s(t) \triangleq \begin{cases} \exp\left[j2\pi\left\{\left(\frac{s}{N_s} - \frac{1}{2}\right)Bt + \frac{B}{2T_s}t^2\right\}\right], & 0 \le t < t_{\mathrm{fold}} \\ \exp\left[j2\pi\left\{\left(\frac{s}{N_s} - \frac{3}{2}\right)Bt + \frac{B}{2T_s}t^2\right\}\right], & t_{\mathrm{fold}} \le t < T_s \end{cases} \tag{1}$$

where $N_s = 2^{SF}$ represents the number of LoRa symbols. Additionally, the symbol duration and the folding time are denoted by $T_s = N_s/B$ and $t_{\mathrm{fold}} = \frac{N_s - s}{B}$, respectively.

The LoRa modulated signal in the discrete-time domain can be obtained by sampling the continuous LoRa signal with the sampling rate of B, which is given by

$$x_s[n] \triangleq x_s(n/B) = \begin{cases} \exp\left[j2\pi\left\{\left(\frac{s}{N_s} - \frac{1}{2}\right)n + \frac{n^2}{2N_s}\right\}\right], & n \in \mathcal{N}_1 \\ \exp\left[j2\pi\left\{\left(\frac{s}{N_s} - \frac{3}{2}\right)n + \frac{n^2}{2N_s}\right\}\right], & n \in \mathcal{N}_2 \end{cases} \tag{2}$$

where $\mathcal{N}_1 = \{0, 1, \cdots, n_{\mathrm{fold}}\}$, $\mathcal{N}_2 = \{n_{\mathrm{fold}}, \cdots, N_s - 1\}$, and $n_{\mathrm{fold}} = N_s - s$ [18]. In this paper, we consider the LoRa modulation in the discrete-time domain given by (2).

1.2.2. Downlink Scenario

We first consider the downlink scenario where the BS transmits LoRa signals to the UAVs. There are K UAVs, each equipped with a single antenna. Additionally, the BS is equipped with M antennas. The downlink channel and beamforming vectors from the UAVs to the BS are denoted by $\mathbf{h}_{\mathrm{d},k} \in \mathbb{C}^{M\times 1}$ and $\mathbf{w}_k \in \mathbb{C}^{M\times 1}$, respectively, for $k = 1, \cdots, K$. Then, the received signal at time slot n is given by

$$y_{\mathrm{d},k}[n] = \mathbf{h}_{\mathrm{d},k}^H[n] \sum_{i=1}^{K} \mathbf{w}_i[n] x_i[n] + z_k[n] \tag{3}$$

where $z_k[n] \sim \mathcal{CN}(0, \sigma^2)$ denotes the received noise at the k-th user. Using the orthogonality property of the LoRa modulated signals (i.e., $\sum_{n=0}^{N-1} x_s[n] x_{s'}^*[n] = 0$ for $0 \leq s \neq s' \leq N_s - 1$ [18]), the corresponding SINR can be derived as

$$\mathrm{SINR}_{\mathrm{d},k}[n] = \frac{|\mathbf{h}_{\mathrm{d},k}^H[n]\mathbf{w}_k[n]|^2}{\sum_{i\neq k} |\mathbf{h}_{\mathrm{d},k}^H[n]\mathbf{w}_i[n]|^2 + \sigma^2} \tag{4}$$

which is described in [22].

In the downlink scenario, for each time slot n, we aim to minimize the transmit power of the BS under the SINR constraints at the UAVs by optimizing the downlink beamforming vectors $\{\mathbf{w}_k[n] : k = 1, \cdots, K\}$, which is formulated as follows:

$$\begin{aligned} (\mathrm{P1}): \quad & \min_{\{\mathbf{w}_k[n]\}_{k=1}^K} \quad \sum_{k=1}^{K} \|\mathbf{w}_k[n]\|^2 \\ & \text{s.t.} \quad \mathrm{SINR}_{\mathrm{d},k}[n] \geq \gamma_{\mathrm{d},k}, \ \forall k \end{aligned} \tag{5}$$

where $\gamma_{\mathrm{d},k}$ denotes the SINR threshold for the k-th UAV. Note that the problem (P1) is a nonconvex optimization problem since the SINR constraints are all nonconvex.

1.2.3. Uplink Scenario

Next, we consider the uplink scenario where the UAVs send their own information to the BS using the LoRa. In the uplink scenario, the received signal at the BS and the corresponding SINR for the k-th UAV are, respectively, given by

$$\mathbf{y}_{\mathrm{u}}[n] = \sum_{k=1}^{K} \sqrt{p_k[n]} \mathbf{h}_{\mathrm{u},k}[n] x_k[n] + \mathbf{z}[n], \tag{6}$$

$$\mathrm{SINR}_{\mathrm{u},k}[n] = \frac{p_k[n]||\mathbf{h}_{\mathrm{u},k}[n]||^2}{\sum_{i\neq k} p_i[n]||\mathbf{h}_{\mathrm{u},i}[n]||^2 + M\sigma^2} \tag{7}$$

where $p_k[n]$, $\mathbf{h}_{\mathrm{u},k}[n] \in \mathbb{C}^{M\times 1}$, and $\mathbf{z}[n]$ denote the transmit power of the k-th UAV, the uplink channel vector from the k-th UAV to the BS, and the noise vector at time slot n, respectively.

In the uplink scenario, for each time slot n, we aim to minimize the total transmit power of the UAVs under the SINR constraints at the BS by optimizing the transmit power $\{p_k[n] : k = 1, \cdots, K\}$ of the UAVs, which is formulated as follows:

$$\begin{aligned} (\mathrm{P2}): \quad & \min_{\{p[n]\}_{k=1}^K} \quad \sum_{k=1}^{K} p_k[n] \\ & \text{s.t.} \quad \mathrm{SINR}_{\mathrm{u},k}[n] \geq \gamma_{\mathrm{u},k}, \ \forall k. \end{aligned} \tag{8}$$

where $\gamma_{\mathrm{u},k}$ is the SINR threshold. Similarly to the downlink scenario, the problem (P2) for the uplink scenario is nonconvex as well.

2. Downlink Beamforming Design and Uplink Power Allocation

2.1. Methodology: Convex Optimization-Based Downlink Beamforming Design and Uplink Power Allocation

In this subsection, we present the conventional approaches for the downlink beamforming design and uplink power allocation via the convex optimization.

2.1.1. Downlink Scenario

Since the denominator of the $\mathrm{SINR}_{\mathrm{d},k}[n]$ in (4) is strictly positive, the constraints of the problem (P1) can be rewritten as follows:

$$\frac{1}{\gamma_{\mathrm{d},k}\sigma^2}|\mathbf{h}_{\mathrm{d},k}^H[n]\mathbf{w}_k[n]|^2 \geq \sum_{i\neq k}\frac{1}{\sigma^2}|\mathbf{h}_{\mathrm{d},k}^H[n]\mathbf{w}_i[n]|^2 + 1. \tag{9}$$

It was shown in [23] that the above inequality can be rewritten as follows:

$$\begin{aligned}\frac{1}{\sqrt{\gamma_{\mathrm{d},k}\sigma^2}}\mathrm{Re}\left\{\mathbf{h}_{\mathrm{d},k}^H[n]\mathbf{w}_k[n]\right\} &\geq \sqrt{\sum_{i\neq k}\frac{1}{\sigma^2}\left|\mathbf{h}_{\mathrm{d},k}^H[n]\mathbf{w}_i[n]\right|^2 + 1} \\ &= \left\|\tfrac{1}{\sigma}\mathbf{h}_{\mathrm{d},1}^H[n]\mathbf{w}_1[n], \quad \cdots, \quad \tfrac{1}{\sigma}\mathbf{h}_{\mathrm{d},k}^H[n]\mathbf{w}_k[n]\right\|_2.\end{aligned} \tag{10}$$

Thus, using (10), the problem (P1) can be reformulated as the following SOCP:

$$\begin{aligned}(\mathrm{P1}'): \quad &\min_{\{\mathbf{w}_k[n]\}_{k=1}^K} \quad \sum_{k=1}^K \|\mathbf{w}_k[n]\|^2 \\ &\text{s.t.} \quad ||\mathbf{h}_{\mathrm{d},k}^T[n]\mathbf{W}[n], \sigma|| \leq \sqrt{1+\frac{1}{\gamma_{\mathrm{d},k}}}\mathbf{h}_{\mathrm{d},k}^T[n]\mathbf{w}_k[n], \ \forall k\end{aligned} \tag{11}$$

where $\mathbf{W}[n] = [\mathbf{w}_1[n], \cdots, \mathbf{w}_K[n]]$. It is worth noting that both the objective function and constraints are convex. Thus, the nonconvex problem (P1) is recast into a convex form in (P1′), which can be solved numerically via convex optimization methods, such as the interior point method [7].

2.1.2. Uplink Scenario

Similarly to in problem (P1), in problem (P2), the SINR constraints become

$$\mathrm{SINR}_{\mathrm{u},k}[n] \geq \gamma_{\mathrm{u},k} \Rightarrow \mathbf{H}[n]\mathbf{p}[n] \preccurlyeq -\sigma^2 \cdot \mathbf{1}_{K\times 1}, \quad \forall k \tag{12}$$

where $\mathbf{H}[n] \in \mathbb{C}^{K\times K}$ and $\mathbf{p}[n] \in \mathbb{R}^{K\times 1}$ are, respectively, defined as

$$\begin{aligned}\mathbf{H}[n] &= \begin{bmatrix} -\frac{1}{\gamma_{\mathrm{u},1}}\|\mathbf{h}_{\mathrm{u},1}[n]\|^2, & \|\mathbf{h}_{\mathrm{u},2}[n]\|^2, & \cdots & \|\mathbf{h}_{\mathrm{u},K}[n]\|^2 \\ \|\mathbf{h}_{\mathrm{u},1}[n]\|^2, & -\frac{1}{\gamma_{\mathrm{u},2}}\|\mathbf{h}_{\mathrm{u},2}[n]\|^2, & \cdots & \|\mathbf{h}_{\mathrm{u},K}[n]\|^2 \\ \vdots & \vdots & \ddots & \vdots \\ \|\mathbf{h}_{\mathrm{u},1}[n]\|^2, & \|\mathbf{h}_{\mathrm{u},2}[n]\|^2, & \cdots & -\frac{1}{\gamma_{\mathrm{u},K}}\|\mathbf{h}_{\mathrm{u},K}[n]\|^2 \end{bmatrix} \\ \mathbf{p}[n] &= [p_1[n], \quad p_2[n], \quad \cdots \quad p_K[n]]^T.\end{aligned} \tag{13}$$

From (12), the problem (P2) can be converted into an LP as follows:

$$\begin{aligned}(\mathrm{P2}'): \quad &\min_{p_k[n]} \quad \mathbf{1}_{K\times 1}^\top \mathbf{p}[n] \\ &\text{s.t.} \quad \mathbf{H}[n]\mathbf{p}[n] \preccurlyeq -\sigma^2 \cdot \mathbf{1}_{K\times 1}.\end{aligned} \tag{14}$$

As a result, (P2′) can be numerically solved via the convex or linear optimization method.

2.2. Methodology: Deep Learning-Based Downlink Beamforming Design and Uplink Power Allocation

2.2.1. Limitations of the Conventional Approaches

The optimization-theoretic approaches described in the previous section yield the solutions in almost all situations (as long as the problems (P1′) and (P2′) are feasible). However, such approaches require high computational complexities increasing proportionally to the total number N_s of time slots, which practically prohibited in the UAV wireless communication system because N_s is typically large (for example, $N_s = 4096$ when $SF = 12$, meaning that the optimization problem (P1′) or (P2′) must be re-solved 4096 times). Specifically, in the downlink, solving the SOCP problem (P1′) requires a large computational complexity of $\mathcal{O}\left(K^{1.5}M^4 \log(1/\epsilon)\right)$ for every time slot n [24], and, thus, the total computational complexity even becomes grower to $\mathcal{O}\left(N_s K^{1.5} M^4 \log(1/\epsilon)\right)$, where ϵ is accuracy for interior-point method (typically, set $\epsilon = 1 \times 10^{-6}$) [25]. Meanwhile, in the uplink, solving the LP problem (P2′) requires a computational complexity of $\mathcal{O}\left(M^2 K \log K \log(1/\epsilon)\right)$ for every time slot n [26], and thus, the total computational complexity even becomes $\mathcal{O}\left(N_s M^2 K \log K \log(1/\epsilon)\right)$.

In order to address such complexity issues, in this paper, we propose a new data-driven cutting-edge approach for the downlink beamforming design and uplink power allocation in the UAV wireless communication system based on deep learning, which requires a low and controllable computational complexity of $\mathcal{O}(K(D_{in}D_1 + \sum_{i=1}^{L-1} D_i D_{i+1} + D_L D_{out}))$ (at the online deployment stage after an offline training), and thus, enables a real-time computation [27]. Here, D_i, D_{in}, and D_{out} denote the number of nodes in the i-th layer, the number of nodes in the input layer, and the number of nodes in the output layer, respectively, of the deep neural network (DNN) constructed in the next section. Additionally, L is the number of hidden layers. It is worth noting that, if the values of D_i's are properly chosen, the proposed scheme requires much lower computational complexity than the conventional scheme (e.g., if we select $D_i, i = 1$ to L that satisfy $\frac{1}{6}\left(D_{in}D_1 + \sum_{i=1}^{L-1} D_i D_{i+1} + D_L D_{out}\right) \geq K^{0.5}M^4$ in the downlink or $\frac{1}{6}\left(D_{in}D_1 + \sum_{i=1}^{L-1} D_i D_{i+1} + D_L D_{out}\right) \geq M^2 \log K$ in the uplink).

In addition, the practical merit of the proposed approach is that the constructed DNN can be *universally* applied to *both* the downlink beamforming design *and* the uplink power allocation (i.e., it is usable regardless of whether the scenario is the downlink or the uplink), although the conventional approach relies particularly on whether the scenario is the downlink or the uplink. To conclude, the proposed scheme has low computational complexity and is thus more efficient compared to the conventional schemes for both scenarios in almost all practical situations (see Tables 1 and 2 for detailed comparisons in various situations. We used bold to the comparatively lower complexity).

Table 1. Computational complexities for the various (M, K) pairs in the uplink.

(M, K)	Conventional Scheme (Uplink)	Proposed Scheme
$(4, 6)$	**448**	7104
$(8, 6)$	**1793**	7872
$(16, 8)$	**11,097**	12,544
$(32, 8)$	44,389	**16,640**
$(64, 10)$	245,760	**31,040**
$(128, 10)$	983,040	**51,520**

Table 2. Computational complexities for the various (M, K) pairs in the downlink.

(M, K)	Conventional Scheme (Downlink)	Proposed Scheme
$(4, 6)$	**22,574**	56,832
$(8, 6)$	361,192	**125,952**
$(16, 8)$	8,897,462	**401,408**
$(32, 8)$	142,359,398	**1,064,960**
$(64, 10)$	3,183,252,921	**3,973,120**
$(128, 10)$	50,930,046,742	**13,189,120**

The network architecture of the proposed scheme will be elaborated in the next section.

2.2.2. Network Architecture

The architecture of the constructed DNN is shown in Figure 2, of which goal is to efficiently compute (or predict) the solution to the problem (P1′) in the downlink or (P2′) in the uplink.

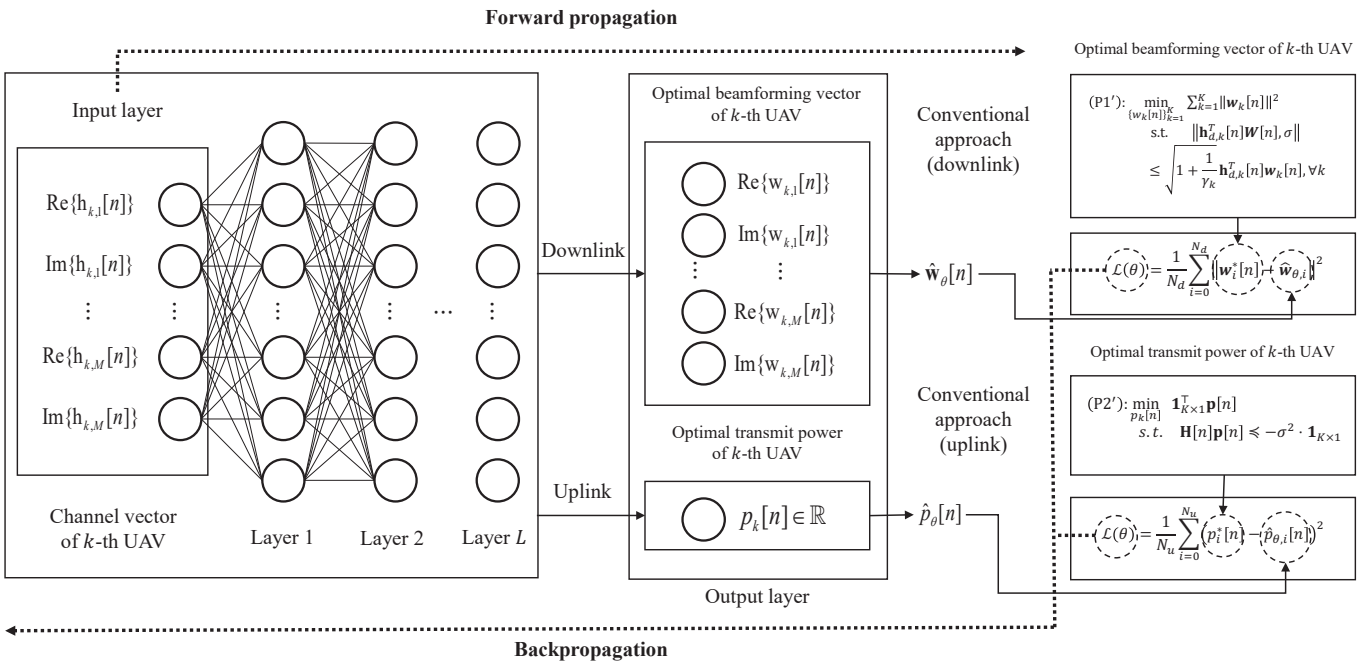

Figure 2. The network structure and loss function of the proposed scheme.

The constructed DNN uses the channel vector between the BS and the k-th UAV as the input and yields the optimal beamforming vector for the k-th UAV in the downlink scenario or optimal transmit power for the k-th UAV in the uplink scenario. Specifically, the input and output of the constructed DNN, respectively, are represented as

$$\begin{aligned} \text{Input} &= \begin{cases} [\mathrm{Re}(\mathbf{h}_{\mathrm{d},k}[n]), \mathrm{Im}(\mathbf{h}_{\mathrm{d},k}[n])]^{\top}, & \text{for the downlink} \\ [\mathrm{Re}(\mathbf{h}_{\mathrm{u},k}[n]), \mathrm{Im}(\mathbf{h}_{\mathrm{u},k}[n])]^{\top}, & \text{for the uplink} \end{cases} \\ \text{Output} &= \begin{cases} \hat{\mathbf{w}}_{k,\theta}[n], & \text{for the downlink} \\ \hat{p}_{k,\theta}[n], & \text{for the uplink} \end{cases} \end{aligned} \tag{15}$$

where $\hat{\mathbf{w}}_{k,\theta}[n]$ and $\hat{p}_{k,\theta}[n]$ are the estimate of the solutions to (P1′) and (P2′) for the k-th UAV, respectively.

The activation function decides whether or not a neuron will be activated or not and transferred to the next layer. It helps in the process of backpropagation because of their differentiable property. During the training process, the loss function is updated, and the activation function makes the gradient descent curves to achieve their local minima. We select the exponential linear unit (ELU) [28] as the activation function, which is a widely adopted activation function to alleviate various practical issues related to training (e.g., vanishing/exploding gradient [29] and dying ReLU problem [30]), which is given by

$$\mathrm{ELU}(x) = \begin{cases} x, & \text{if } x > 0 \\ \mu(\exp(x) - 1), & \text{if } x \leq 0 \end{cases} \tag{16}$$

where x denotes an input feature, and μ represents a hyperparameter that controls the saturation value.

2.2.3. Training Procedure

The constructed DNN is trained in a supervised manner. Specifically, let $\mathbf{w}_k^*[n]$ and $p_k^*[n]$ be the solutions to (P1′) and (P2′) for the k-th UAV, respectively. Then, for the training of the constructed DNN, we take the label as $\mathbf{w}_k^*[n]$ in the downlink and $p_k^*[n]$ in the uplink.

For prediction with the minimum error, we select mean squared error (MSE) between the label and the output of the constructed DNN as the loss function as follows:

$$\mathcal{L}(\theta) = \begin{cases} \frac{1}{N_d}\sum_{i=0}^{N_d} \|\mathbf{w}_i^*[n] - \hat{\mathbf{w}}_{\theta,i}[n]\|^2, & \text{for the downlink} \\ \frac{1}{N_u}\sum_{i=0}^{N_u} \left(p_i^*[n] - \hat{p}_{\theta,i}[n]\right)^2, & \text{for the uplink} \end{cases} \tag{17}$$

where θ denotes the parameters of the constructed network. Additionally, N_d, and N_u denote the number of training samples for the downlink and the number of training samples for the uplink, respectively.

The weight update through the gradient descent is known to be effective and widely adopted [31]. The update rule of the gradient descent algorithm is described as follows:

$$\theta_{t+1} \leftarrow \theta_t - \alpha \nabla_{\theta_t} \mathcal{L}(\theta_t) \tag{18}$$

where $\alpha > 0$ is the learning rate, which determines the step size of the update.

For the UAV wireless communication, it is utmost important to realize good generalization behavior and fast convergence rate. Toward these goals, we adopt Nadam [31], which is a combination of nesterov accelerated gradient (NAG) [32] and adaptive moment estimation (Adam) [33] algorithm, in which the gradient can be expressed as

$$\theta_{t+1} \leftarrow \theta_t - \frac{\alpha}{\sqrt{\hat{\upsilon}_t} + \zeta}\left(\beta \hat{m}_t + \frac{(1-\beta)\nabla_{\theta_t}\mathcal{L}(\theta_t)}{1-\beta^t}\right) \tag{19}$$

where β, $\hat{m}$, and $\hat{\upsilon}$ denote the decay rate of the first momentum vector, the bias-corrected first momentum vector, and the bias-corrected second momentum vector, respectively. Additionally, ζ is added to prevent the denominator from becoming zero (typically, set $\zeta = 1 \times 10^{-6}$).

3. Numerical Results

In this section, we compare the performance of the proposed scheme to that of the conventional approaches through the numerical results. In the simulation, we consider the LoRa signals with $B = 500$ kHz and Rician fading channel model which is given by

$$\mathbf{h}[n] = (\kappa/(1+\kappa))^{(1/2)}\mathbf{h}^{\mathrm{LOS}}[n] + (1/(1+\kappa)^{(1/2)}\mathbf{h}^{\mathrm{scatter}}[n] \tag{20}$$

with the K-factor set to $\kappa = 13$ dB, where the first term and the second term denote the line of sight (LOS) component and the scattering component, respectively. Additionally, the

solutions to (P1′) and (P2′) are obtained via the MATLAB CVX solver [34]. The batch size and the learning rate for the proposed scheme are set to 1 and 0.01, respectively. In addition, the constructed DNN consists of three hidden layers each with 16, 32, and 16 nodes. The simulations are conducted in the range of 0 dB $\leq \gamma_{\mathrm{d},k} \leq$ 50 dB in the downlink and 0 dB $\leq \gamma_{\mathrm{u},k} \leq$ 0.5 dB in the uplink, respectively. Additionally, the velocities of all UAVs are set to be the same as v and the SINR threshold for both the downlink and uplink scenarios is set to $\gamma = \gamma_{\mathrm{d},k} = \gamma_{\mathrm{u},k}, \forall k$.

In Figure 3, we plot the computational complexities of the conventional scheme and the proposed scheme with a fixed number of antennas of BS $M = 32$. From Figure 3, we can observe that the proposed scheme has lower complexity than conventional optimization based scheme for each scenario.

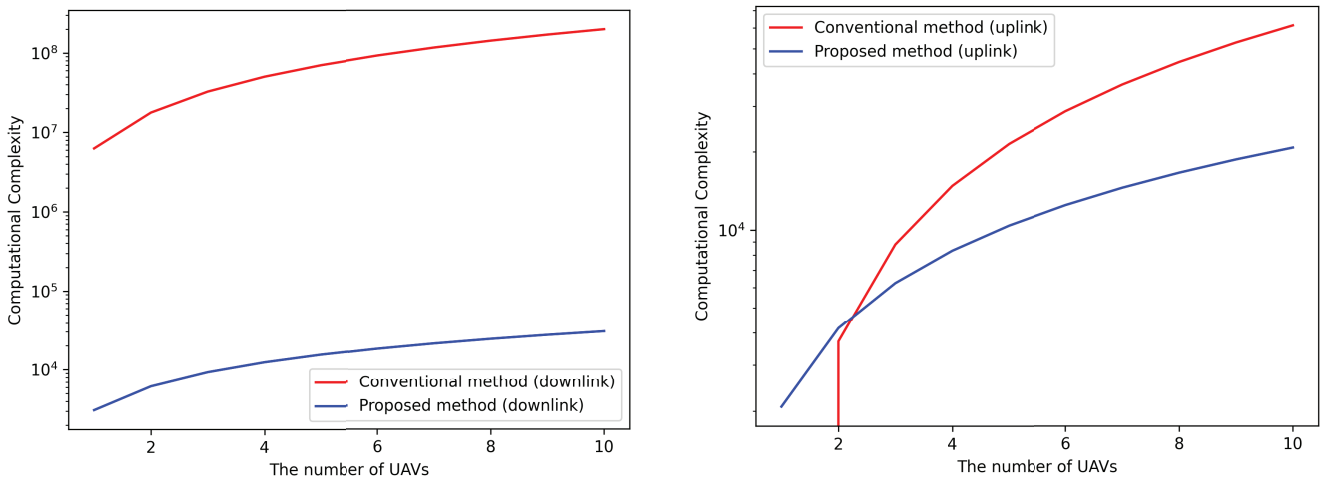

(**a**) Downlink (**b**) Uplink

Figure 3. Computational complexities of the conventional scheme and the proposed scheme.

In Figure 4, we plot learning curves of the proposed scheme in the downlink for $K = 2$ and $K = 5$, respectively, when the UAVs' velocity v is set to 160 km/h. From Figure 4, we can observe that during the training and validation, the MSE (i.e., loss function) tends to decrease as the epoch increases, meaning that the proposed scheme learns the solution to (P1′) well. Additionally, one can see that the MSE for the validation tends to be below the training curve due to the use of Dropout [35]. In the simulations, the dropout rates for each hidden layer L_1, L_2, and L_3 were set to 0.2, 0.3, and 0.3, respectively.

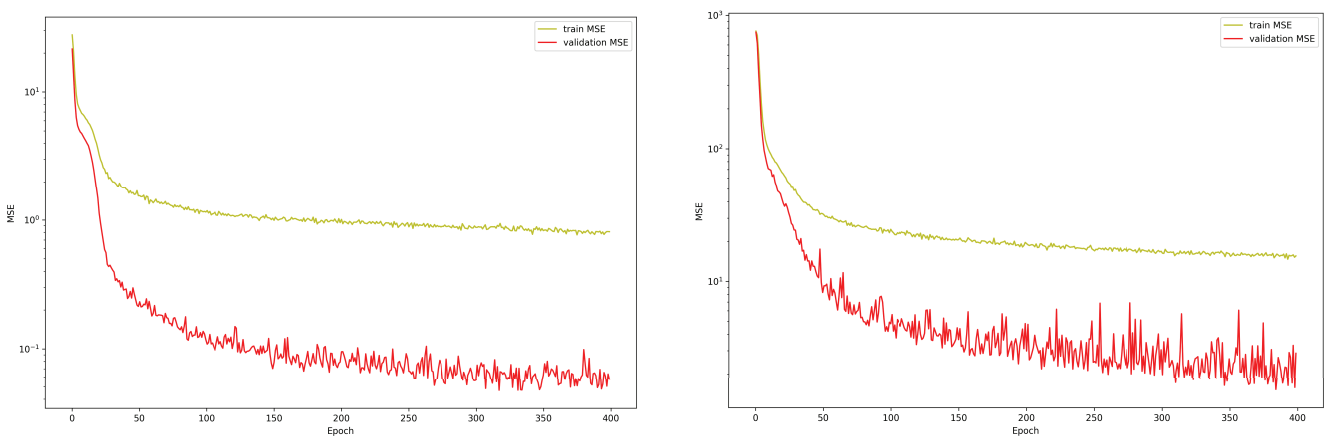

(**a**) $K = 2$ (**b**) $K = 5$

Figure 4. Learning curve of the proposed scheme for the downlink with v = 160 km/h.

In Figure 5, the minimum transmit power is shown versus the SINR threshold γ for the downlink to compare the performance of the proposed scheme with the solution to (P1′), where we set $v = 160$ km/h. From the Figure 5, we can observe that the constructed DNN accurately predicts the solution to (P1′) over the entire regime of γ except for the low regime of γ.

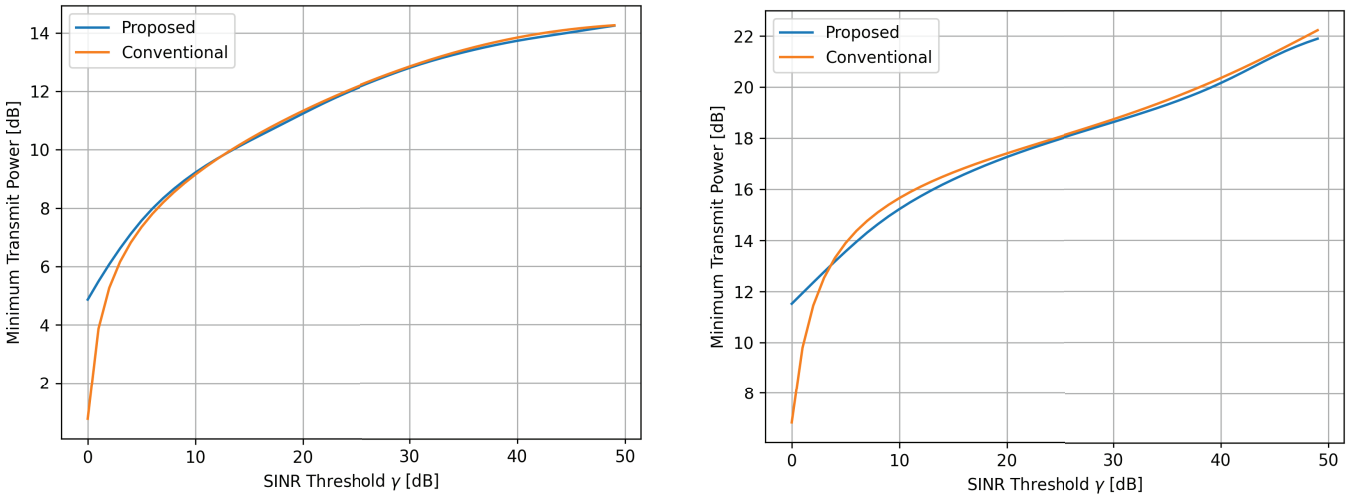

(**a**) $K = 2$ (**b**) $K = 5$

Figure 5. Minimum transmit power versus the SINR threshold for the downlink with $v = 160$ km/h.

Figure 6 shows the minimum transmit power versus the SINR threshold γ in the downlink for the same simulation setup as in Figure 5 except that v is set to 300 km/h. From the Figure 6, one can see the similar behaviors as in the Figure 5. Specifically, the constructed DNN is able to precisely approximate the solution to (P1′) when the value of γ is between 10 dB and 50 dB, i.e., 10 dB $\leq \gamma \leq$ 50 dB, while it tends to slightly overestimate the solution to (P1′) when the value of γ is below 10 dB, i.e., $\gamma <$ 10 dB. Additionally, From Figures 5 and 6, we can further observe that the proposed scheme works robustly to the velocity variation of the UAVs, i.e., the predicted result well approximates the solution to (P1′) regardless of the UAVs' velocity.

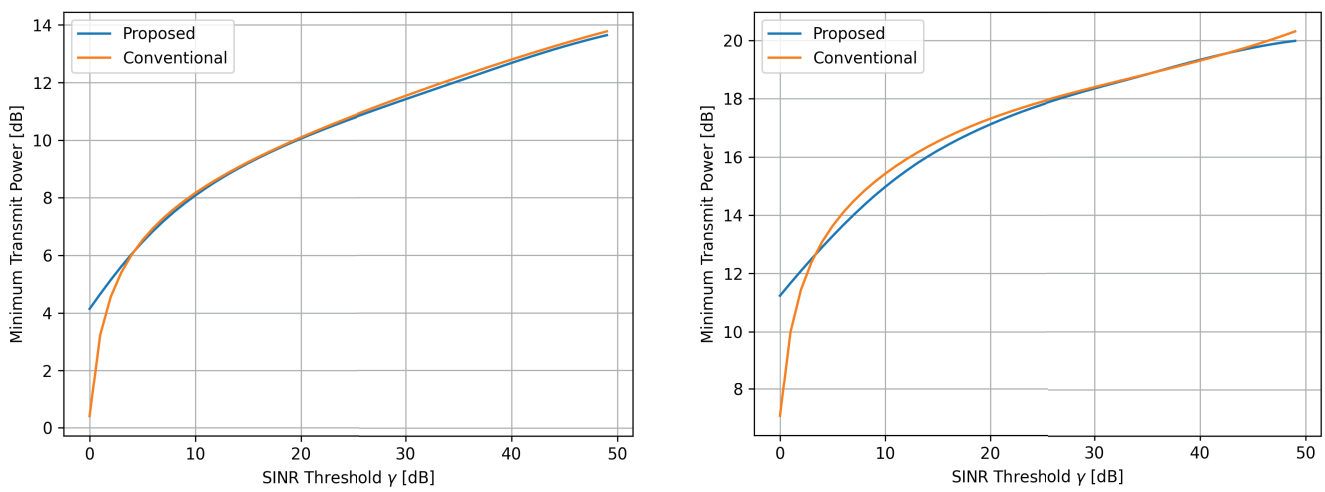

(**a**) $K = 2$ (**b**) $K = 5$

Figure 6. Minimum transmit power versus the SINR threshold for the downlink with $v = 300$ km/h.

In Figure 7, we plot the learning curves of the proposed scheme in the uplink when $v = 160$ km/h with $K = 2$ and $K = 5$, respectively. From these results, one can see that the losses and MSEs of the proposed scheme gradually decrease. Additionally, for the same reason as in the Figure 4 (i.e., due to the use of Dropout), the validation curves tend to be below the training curves.

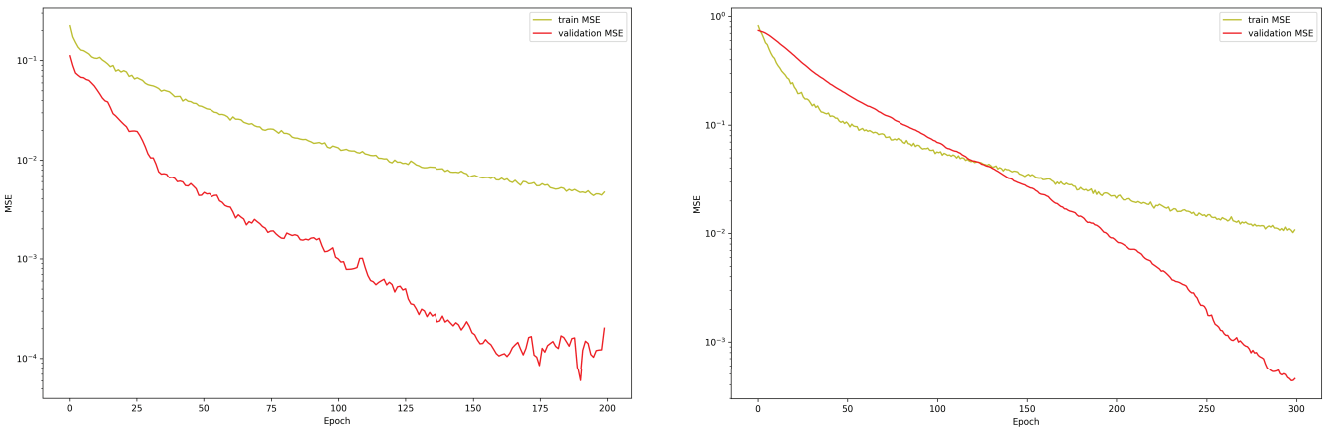

(**a**) $K = 2$ (**b**) $K = 5$

Figure 7. Learning curve of the proposed scheme for the uplink with $v = 160$ km/h.

Figure 8 depicts the minimum transmit power versus the SINR threshold γ for the uplink when $v = 160$ km/h. From the Figure 8, one can see that the constructed DNN well approximates the solution to (P2′) when 0.1 dB $\leq \gamma \leq$ 0.5 dB while it tends to slightly overestimate when $\gamma <$ 0.1 dB.

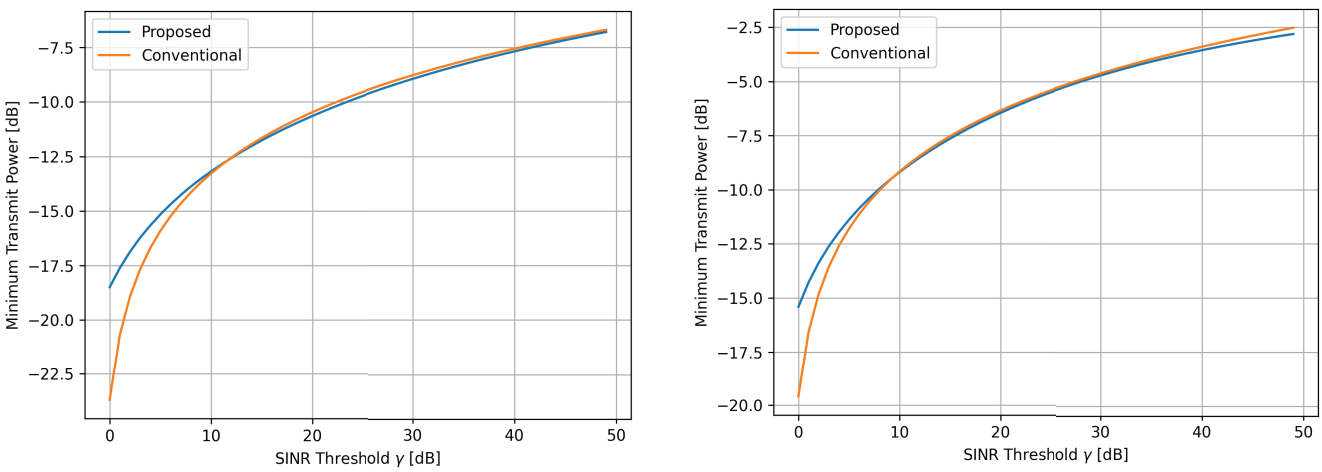

(**a**) $K = 2$ (**b**) $K = 5$

Figure 8. Minimum transmit power versus the SINR threshold for the uplink with $v = 160$ km/h.

Figure 9 shows the performance of the proposed scheme in the uplink for the same simulation setup as in Figure 8 except that v is set to 300 km/h. From Figure 9, we can also observe that the constructed DNN precisely approximates the solution to (P2′) when 0.1 dB $\leq \gamma \leq$ 0.5 dB, while it tends to slightly overestimate the solution to (P2′) otherwise.

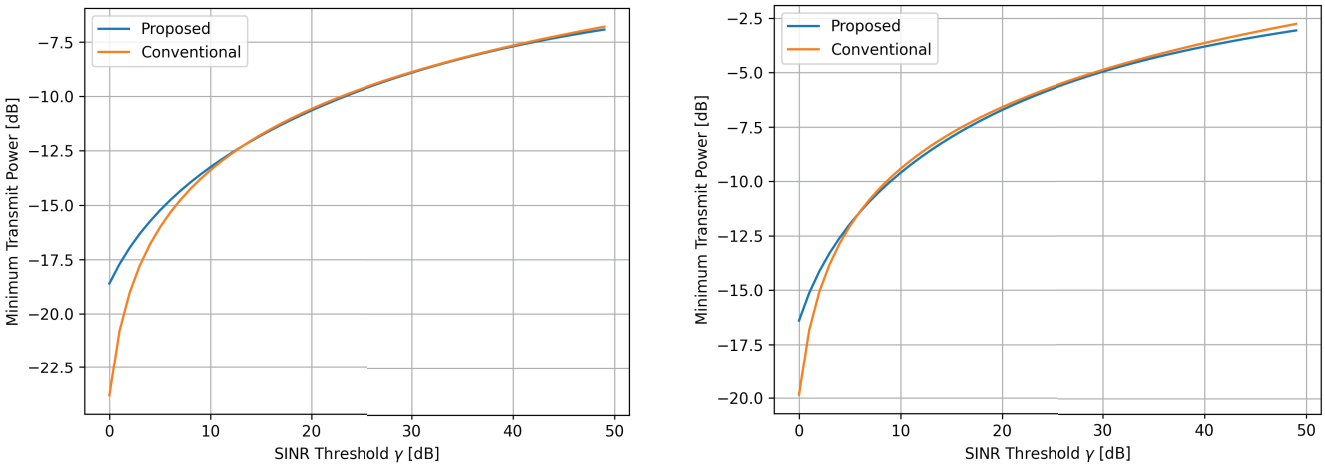

(**a**) $K = 2$ (**b**) $K = 5$

Figure 9. Minimum transmit power versus the SINR threshold for the uplink with $v = 300$ km/h.

4. Conclusions

In this paper, we proposed the universal and efficient DL-based scheme to predict the optimal beamforming vector in the downlink scenario or the transmit power allocation in the uplink scenario with very low computational complexity. We trained the constructed DNN to minimize the MSE-based loss function. The numerical results showed that the proposed scheme could precisely approximate the solutions (i.e., labels) with low computational complexity. An important future work for UAV wireless communications is to maximize the achievable rate using the proposed scheme.

Author Contributions: Conceptualization and methodology, Y.-R.K. and J.-H.P.; validation and formal analysis, Y.-R.K. and J.-H.P.; investigation and resources, D.-W.L. and K.-M.K.; writing—original draft preparation, Y.-R.K. and J.-H.P.; writing—review and editing, supervision, and project administration, J.-M.K. and D.-W.L. All authors have read and agreed to the published version of the manuscript.

Funding: This work was supported by the ICT R&D program of MSIT/IITP. [2019-0-00499, Development of Identification and Frequency Management Technology of Small Drones at Low Altitude].

Institutional Review Board Statement: Not applicable.

Informed Consent Statement: Not applicable.

Data Availability Statement: Not applicable.

Conflicts of Interest: The authors declare no conflict of interest.

Abbreviations

The following abbreviations are used in this manuscript:

Adam	Adaptive Moment Estimation
BS	Base Station
CSI	Channel State Information
DL	Deep Learning
DNN	Deep Neural Network
ELU	Exponential Linear Unit
IoT	Internet of Things
LoRa	Long Range
LP	Linear Programming
LPWAN	Low-Power Wide-Area Network

MSE	Mean Squared Error
NAG	Nesterov Accelerated Gradient
QoS	Quality of Service
SF	Spreading Factor
SINR	Signal-to-Interference-plus-Noise Ratio
SOCP	Second-Order Cone Programming
UAV	Unmanned Aerial Vehicle

References

1. Shakhatreh, H.; Sawalmeh, A.H.; Al-Fuqaha, A.; Dou, Z.; Almaita, E.; Khalil, I.; Othman, N.S.; Khreishah, A.; Guizani, M. Unmanned aerial vehicles (UAVs): A survey on civil applications and key research challenges. *IEEE Access* **2019**, *7*, 48572–48634. [CrossRef]
2. Zeng, Y.; Zhang, R.; Lim, T.J. Wireless communications with unmanned aerial vehicles: Opportunities and challenges. *IEEE Commun. Mag.* **2016**, *54*, 36–42. [CrossRef]
3. Mozaffari, M.; Saad, W.; Bennis, M.; Nam, Y.H.; Debbah, M. A tutorial on UAVs for wireless networks: Applications, challenges, and open problems. *IEEE Commun. Surv. Tutor.* **2019**, *21*, 2334–2360. [CrossRef]
4. Augustin, A.; Yi, J.; Clausen, T.; Townsley, W.M. A study of LoRa: Long range & low power networks for the internet of things. *Sensors* **2016**, *16*, 1466.
5. Raza, U.; Kulkarni, P.; Sooriyabandara, M. Low power wide area networks: An overview. *IEEE Commun. Surv. Tutor.* **2017**, *19*, 855–873. [CrossRef]
6. Kang, J.M.; Lim, D.W.; Kang, K.M. On the LoRa Modulation for IoT: Optimal Preamble Detection and Its Performance Analysis. *IEEE Internet Things J.* **2021**, *9*, 4973–4986. [CrossRef]
7. Yu, W.; Lan, T. Transmitter optimization for the multi-antenna downlink with per-antenna power constraints. *IEEE Trans. Signal Process.* **2007**, *55*, 2646–2660. [CrossRef]
8. Zhu, J.; Wang, J.; Huang, Y.; Navaie, K.; Ding, Z.; Yang, L. On optimal beamforming design for downlink MISO NOMA systems. *IEEE Trans. Veh. Technol.* **2020**, *69*, 3008–3020. [CrossRef]
9. Huang, Y.; Zhou, L. MISO NOMA downlink beamforming optimization with per-antenna power constraints. *Signal Process.* **2021**, *179*, 107828. [CrossRef]
10. Van Chien, T.; Björnson, E.; Larsson, E.G. Joint power allocation and user association optimization for massive MIMO systems. *IEEE Trans. Wirel. Commun.* **2016**, *15*, 6384–6399. [CrossRef]
11. Zuo, H.; Tao, X. Power allocation optimization for uplink non-orthogonal multiple access systems. In Proceedings of the 2017 9th International Conference on Wireless Communications and Signal Processing (WCSP), Nanjing, China, 11–13 October 2017; pp. 1–5. [CrossRef]
12. Tan, F.; Lv, T.; Yang, S. Power allocation optimization for energy-efficient massive MIMO aided multi-pair decode-and-forward relay systems. *IEEE Trans. Commun.* **2017**, *65*, 2368–2381.
13. Huang, H.; Peng, Y.; Yang, J.; Xia, W.; Gui, G. Fast beamforming design via deep learning. *IEEE Trans. Veh. Technol.* **2019**, *69*, 1065–1069. [CrossRef]
14. Luijten, B.; Cohen, R.; de Bruijn, F.J.; Schmeitz, H.A.; Mischi, M.; Eldar, Y.C.; van Sloun, R.J. Deep learning for fast adaptive beamforming. In Proceedings of the ICASSP 2019—2019 IEEE International Conference on Acoustics, Speech and Signal Processing (ICASSP), Brighton, UK, 12–17 May 2019; pp. 1333–1337.
15. Xie, B.; Yin, Y.; Xiong, J. Pushing the Limits of Long Range Wireless Sensing with LoRa. *Proc. ACM Interact. Mob. Wearable Ubiquitous Technol.* **2021**, *5*, 1–21. [CrossRef]
16. Nguyen, T.T.; Nguyen, H.H.; Barton, R.; Grossetete, P. Efficient design of chirp spread spectrum modulation for low-power wide-area networks. *IEEE Internet Things J.* **2019**, *6*, 9503–9515. [CrossRef]
17. Vangelista, L. Frequency Shift Chirp Modulation: The LoRa Modulation. *IEEE Signal Process. Lett.* **2017**, *24*, 1818–1821. [CrossRef]
18. Chiani, M.; Elzanaty, A. On the LoRa Modulation for IoT: Waveform Properties and Spectral Analysis. *IEEE Internet Things J.* **2019**, *6*, 8463–8470. [CrossRef]
19. Bernier, C.; Dehmas, F.; Deparis, N. Low complexity LoRa frame synchronization for ultra-low power software-defined radios. *IEEE Trans. Commun.* **2020**, *68*, 3140–3152. [CrossRef]
20. Xhonneux, M.; Bol, D.; Louveaux, J. A low-complexity synchronization scheme for LoRa end nodes. *arXiv* **2019**, arXiv:1912.11344.
21. Ghanaatian, R.; Afisiadis, O.; Cotting, M.; Burg, A. LoRa digital receiver analysis and implementation. In Proceedings of the ICASSP 2019—2019 IEEE International Conference on Acoustics, Speech and Signal Processing (ICASSP), Brighton, UK, 12–17 May 2019; pp. 1498–1502.
22. Schubert, M.; Boche, H. Solution of the multiuser downlink beamforming problem with individual SINR constraints. *IEEE Trans. Veh. Technol.* **2004**, *53*, 18–28. [CrossRef]
23. Björnson, E.; Bengtsson, M.; Ottersten, B. Optimal Multiuser Transmit Beamforming: A Difficult Problem with a Simple Solution Structure [Lecture Notes]. *IEEE Signal Process. Mag.* **2014**, *31*, 142–148. [CrossRef]
24. Li, Y.; Jiang, M.; Zhang, Q.; Qin, J. Joint beamforming design in multi-cluster MISO NOMA reconfigurable intelligent surface-aided downlink communication networks. *IEEE Trans. Commun.* **2020**, *69*, 664–674. [CrossRef]

25. Luo, Z.Q.; Yu, W. An introduction to convex optimization for communications and signal processing. *IEEE J. Sel. Areas Commun.* **2006**, *24*, 1426–1438.
26. Morin, T.; Prabhu, N.; Zhang, Z. Complexity of the gravitational method for linear programming. *J. Optim. Theory Appl.* **2001**, *108*, 633–658. [CrossRef]
27. Freire, P.J.; Osadchuk, Y.; Spinnler, B.; Napoli, A.; Schairer, W.; Costa, N.; Prilepsky, J.E.; Turitsyn, S.K. Performance versus complexity study of neural network equalizers in coherent optical systems. *J. Light. Technol.* **2021**, *39*, 6085–6096. [CrossRef]
28. Clevert, D.A.; Unterthiner, T.; Hochreiter, S. Fast and accurate deep network learning by exponential linear units (elus). *arXiv* **2015**, arXiv:1511.07289.
29. Bengio, Y.; Simard, P.; Frasconi, P. Learning long-term dependencies with gradient descent is difficult. *IEEE Trans. Neural Netw.* **1994**, *5*, 157–166. [CrossRef]
30. Lu, L.; Shin, Y.; Su, Y.; Karniadakis, G.E. Dying relu and initialization: Theory and numerical examples. *arXiv* **2019**, arXiv:1903.06733.
31. Ruder, S. An overview of gradient descent optimization algorithms. *arXiv* **2016**, arXiv:1609.04747.
32. Botev, A.; Lever, G.; Barber, D. Nesterov's accelerated gradient and momentum as approximations to regularised update descent. In Proceedings of the 2017 International Joint Conference on Neural Networks (IJCNN), Anchorage, AK, USA, 14–19 May 2017; pp. 1899–1903.
33. Kingma, D.P.; Ba, J. Adam: A method for stochastic optimization. *arXiv* **2014**, arXiv:1412.6980.
34. Grant, M.; Boyd, S. *CVX: Matlab Software for Disciplined Convex Programming*; Version 2.1; 2014. Available online: http://cvxr.com/cvx/citing/ (accessed on 17 April 2022).
35. Srivastava, N.; Hinton, G.; Krizhevsky, A.; Sutskever, I.; Salakhutdinov, R. Dropout: A simple way to prevent neural networks from overfitting. *J. Mach. Learn. Res.* **2014**, *15*, 1929–1958.